Fully Integrated Magnetically Actuated Micromachined Relays

William P. Taylor, *Member, IEEE,* Oliver Brand, and Mark G. Allen, *Member, IEEE*

***Abstract*— A fully integrated magnetically actuated micromachined relay has been successfully fabricated and tested. This particular device uses a single-layer coil to actuate a movable upper magnetically responsive platform. The minimum current for actuation was 180 mA, resulting in an actuation power of 33 mW. Devices have been tested which can make and break 1.2 A of current through the relay contacts when the relay is electromagnetically switched. Operational lifetimes in excess of 850 000 operations have been observed. Contact resistances as low as 22.4 mΩ have been observed under electromagnetic actuation. Magnetic and structural finite-element (FE) simulations have been performed using ANSYS to calculate both the actuation and contact forces. [288]**

***Index Terms*— Electromagnetic, magnetic, micromachined, relay, switch.**

I. Introduction

ELECTROMECHANICAL relays remain widely used for a number of applications including automotive control circuitry, test equipment, and the switching of high-frequency signals. The manufacturing processes used to produce electromechanical relays have historically been serial in nature. Solid-state relays (SSR's) have been one solution to this production problem. SSR's allow for devices to be batch fabricated, however, they also may have higher offset voltage injection, lower maximum off-state resistance, and higher contact power dissipation than their electromagnetic counterparts. For those reasons, electromagnetic relays remain widely used for many applications. Micromachined relays are produced by the application of batch fabrication techniques to electromechanical relays. This approach attempts to combine the best attributes of both electromechanical relays and SSR's, namely, the smaller size of solid-state devices and the increased off resistance and lower on resistance that is more typical of electromechanical relays. Micromachined relays may also allow for the interconnection of large relay arrays during fabrication, thus reducing other fabrication steps currently needed for relay arrays.

Microfabrication techniques have been used for the fabrication of electromechanical relays for many years. Electrostatically actuated microrelays were demonstrated in 1979 [1]. Those devices used metallic contact materials to reduce the contact resistance and increase the current carrying capacity. Since that time, polysilicon electrostatic microrelays on CMOS have been demonstrated [2], [3]. These devices had a relatively low carry current of approximately 10 mA. Other versions of electrostatic microrelays have also been demonstrated and have shown lower contact resistance through the use of metallic contact materials [4]–[7]. Another electrostatic device has also been reported with actuation voltages from 30 to 400 V [8] and a switched current of 10 mA. One electrostatically actuated device reported lifetimes in excess of 10^8 [5]. A recent electrostatic microrelay [9] displayed the ability to actuate with less than 24 V and was able to switch currents up to 200 mA.

Mercury can be used in electromechanical relays to improve lifetimes by reducing the contact wear and arcing effects. A thermally driven microrelay with mercury contacts has been demonstrated [10]. This device had contact resistance lower than 1 Ω, with a maximum carry current of 20 mA.

In many applications, such as integrated circuit test equipment or automotive environments, a low actuation voltage may be desirable to reduce noise or eliminate the need for voltage converters. Many of these environments allow for high currents to be used at these low voltages. Magnetically driven microrelays are very desirable in such an environment as they are compatible with these requirements. Previously reported magnetic microrelays do not have fully integrated coils or magnetic components [11]–[13]. The schemes presented have used either an external electromagnet [11], [12] to actuate a movable member or an integrated heating element [13] to demagnetize portions of a magnetic circuit, which thereby causes the device to change state toward another magnetized region, pulling the contacting elements apart. The use of an external coil reduces the benefits of batch fabrication by requiring some other assembly and does not allow for the minimum device size to be achieved, as the coils are wound using standard winding techniques. The use of thermal actuation schemes results in relatively large forces, but will tend to increase the switching time. Thermal actuation may also induce noise voltages in the relay contacts due to thermal voltage generation effects.

Our approach has been to use a fully integrated magnetic actuation design to realize integrated microrelays. Previously, we reported a fully integrated magnetically actuated micromachined relay [14], which demonstrated the ability of such a device to be produced. The use of a fully integrated mag-

Manuscript received August 1, 1997; revised February 13, 1998. Subject Editor, W. Benecke. This work was supported by the Microelectronics Research Center, Georgia Institute of Technology.

W. P. Taylor is with Teledyne Relays, Hawthorne, CA 90250-3384 USA.

O. Brand is with the Physical Electronics Laboratory, ETH Zurich, Switzerland.

M. G. Allen is with the School of Electrical and Computer Engineering, Georgia Institute of Technology, Atlanta, GA 30332-0250 USA (e-mail: mallen@ece.gatech.edu).

Publisher Item Identifier S 1057-7157(98)03575-6.

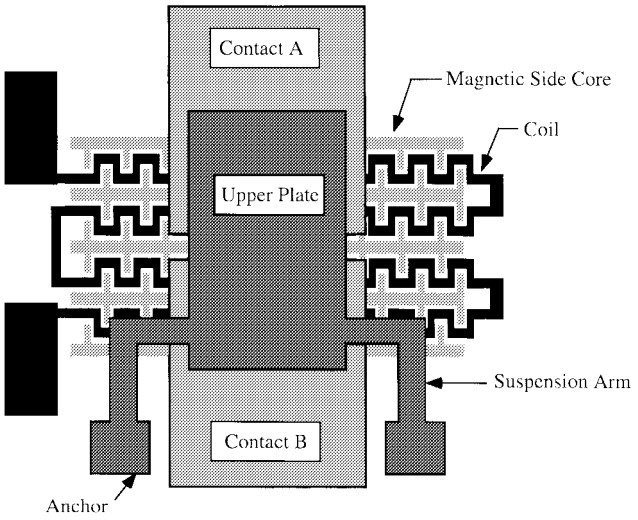

Fig. 1. Schematic overhead view of the microrelay, illustrating the relative positions of the upper movable plate, contacts, side cores, and coils.

netically actuated microrelay design has several advantages. Minimum-sized relays may be obtained, and the devices do not require any assembly of a coil to an actuator plate, thus allowing the maximum advantages of batch fabrication to be realized. By using a magnetic actuation approach the switching speeds are not limited due to thermal time constants. The use of a low-temperature fabrication process (less than 250°C) allows for the devices to be used in packaging technologies, or to be postprocessed with silicon circuitry underneath the microrelay. Another advantage of using a silicon substrate may be the integration of protection diodes across the microrelay coils. Thus, the total number of components on a printed wiring board, or other substrate, e.g., a multichip module, may be reduced.

II. Device Concept

In the design of these microrelays, a single-layer coil was used to reduce fabrication complexity and eliminate the via connections required in a multilayer coil. Elimination of the via connections combined with the meander nature of this coil design results in a lower coil resistance when compared to typical planar spiral coils [15]. Fig. 1 shows a schematic view of a cantilever type normally open microrelay.

The operation of the microrelay is similar to other normally open electromagnetic relays with the exception that the magnetic flux is distributed rather than additive as is the case with most conventional electromagnetic relays. Fig. 2 shows a schematic of the flux patterns and how the flux adds in adjacent-side core areas. The device actuates by passing a current of sufficient magnitude through the coil and generating a magnetic flux which is concentrated by the lower and side magnetic cores. The magnetic flux then flows through the magnetic gap (consisting of the air gap between the contacts and the upper movable plate and the distance from the side core to the top of the contacts) and into the upper magnetic plate. The flux then propagates along the upper magnetic plate to the area over the next side core, where the flux again passes through the magnetic gap and into the adjacent side core on the other side of the coil. The magnetic flux thus generates a force on the upper magnetic plate, resulting in motion of the upper plate toward the electromagnet. When the upper magnetic plate moves down toward the electromagnet, it encounters the two contacts (contacts A and B), which stop its motion. Since the upper plate is conductive, a current can flow from one contact (contact A) through the upper plate and into the other contact (contact B). When the current in the coil is discontinued, the mechanical restoring forces of the upper plate suspension arms are sufficient to pull the upper plate off of the contacts. When the plate is pulled off of the contacts, the current through the contacts is discontinued and the relay is again in the "OFF" state.

III. Fabrication

The microrelay fabrication is based on standard polyimide mold electroplating techniques [16] and consists of an integrated planar meander coil and a pair of relay contacts positioned above the coil. A movable magnetic plate is surface micromachined above the contacts and connects the two contacts when coil current is applied to the electromagnet. Fig. 3 shows a schematic representation of the fabrication sequence.

The fabrication begins with the deposition of a seed layer on the substrate, which is coated with a polymer, such as polyimide. The polymer is patterned and etched with a technique such as plasma etching to form a polymer mold for the subsequent electroplating of the lower magnetic core with a nickel–iron alloy [17]. An insulation layer is deposited over the lower magnetic core, and a seed layer is deposited for the electrodeposition of the coils. The coils are patterned and electroplated through a photoresist mold. Afterwards the photoresist layer and the coil seed layer are removed, which electrically isolates the coil windings from each other. Another polymer insulation layer is deposited. The patterns for the side cores are defined using a plasma technique down to the lower magnetic core. The side magnetic cores are electroplated through the polymer insulation mold. At this point, the electromagnet fabrication is complete, and the entire electromagnet is insulated and planarized using a polymer material. A seed layer is deposited over the electromagnet, and the contacts are patterned and electroplated through a photoresist mold. The photoresist mold and seed layer are removed. A photoresist sacrificial layer is deposited over the contacts and patterned. The upper magnetic plate is electrodeposited over the photoresist sacrificial layer after deposition of the seed layer and patterning of a second photoresist layer. The upper plate photoresist plating mold and seed layer are removed sequentially. The final process step of the fabrication is the removal of the photoresist sacrificial layer and cleaning of the contacts. The devices then are ready to be used as microrelays. Fig. 4 is a photomicrograph of a completed microrelay.

The fabrication temperatures are important for micromagnetic devices as subsequent processing temperature will affect the magnetic properties of the materials deposited previously. For electrodeposited permalloy films, similar to the ones used in the devices described in this paper, the residual stress in

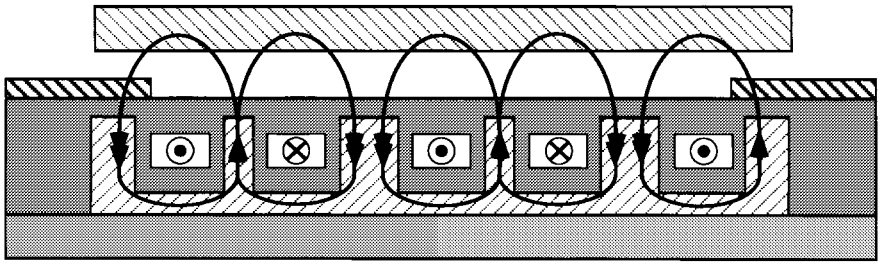

Fig. 2. Schematic side view of the microrelay, showing a conceptual view of the flux patterns generated by this microrelay geometry.

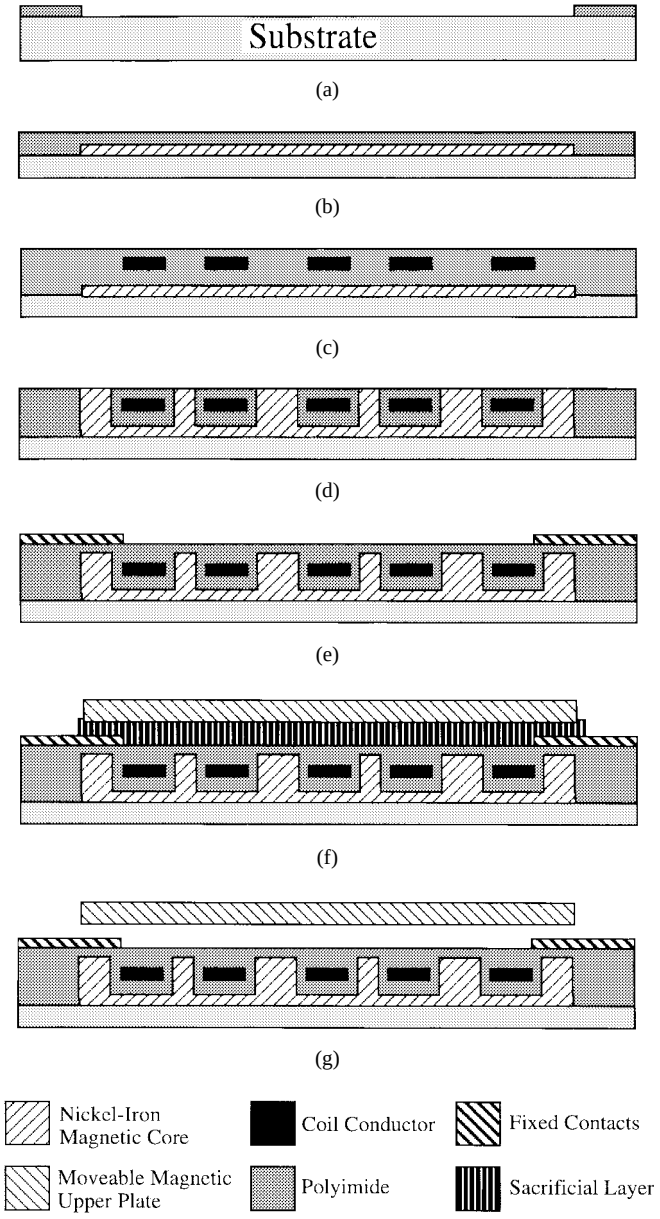

Fig. 3. A side-view schematic of the fabrication process used to produce microrelays. (a) After lower core polymer mold deposition. (b) Insulated lower magnetic core. (c) After coil electroplating and insulation. (d) After side magnetic core electrodeposition. (e) After deposition of contacts over the electromagnet. (f) After plating of the upper movable magnetic plate. (g) The completed microrelay after photoresist sacrificial layer has been removed.

the films increases with exposure to temperatures above the temperature during electrodeposition [18], [19]. This behavior differs from the behavior observed in bulk materials, where the process of annealing is typically used to reduce the residual stress in the material. These film characteristics must be taken into account when designing the fabrication process for any micromagnetic device and especially one where the moving member is made of an electroplated film.

IV. Theoretical Analysis

Previously, we reported a simple theoretical model to describe the microrelay actuation based on reluctance theory [14]. The use of such models are convenient as general design guidelines, but these models may lack the necessary accuracy for full design optimization. As discussed in [20], this is due to the geometrical influences of the micromachined device where the air-gap reluctances become comparable to those of the magnetic core. In such a case, the reluctance of the magnetic cores should not be neglected as is the case for a simple reluctance model. More complex reluctance models may be derived that more accurately represent these effects. However, due to the difficulty in quantitatively incorporating fringing effects into many reluctance-type models, a finite-element (FE) method is preferable.

In order to obtain a more detailed understanding of the microrelay, the basic structure has been analyzed using the general-purpose FE software ANSYS 5.2. Both two-dimensional (2-D) and three-dimensional (3-D) magnetic analyses have been performed to obtain the forces acting on the magnetic upper plate of the microrelay. The results of the simplified 2-D magnetic analysis can be directly compared with the analytical results obtained from the reluctance theory. However, a 2-D analysis is required to more accurately model the characteristics of the actual microrelay structures with their zig–zag coils. The final deflection of the upper plate due to the magnetic forces and the resulting contact forces have been calculated in a subsequent nonlinear structural analysis.

The 2-D magnetic analysis simulates a magnetic actuator with parallel infinitely long current conducting lines. The current direction (either into or out of the plane) alternates from copper line to copper line. Due to symmetry reasons, only a section of the coil consisting of two current lines had to be modeled. The basic repeating unit of the 2-D simulation extends from the center of one current line to the center of the next current line with the same current direction (see Fig. 5). A flux-normal boundary condition (i.e., no flux parallel to the boundary) was applied along the boundaries to the neighboring coil elements. *Eight-node 2-D magnetic solid* elements were used to model the relay structure and the surrounding air. *2-D infinite boundary* elements were incorporated to model

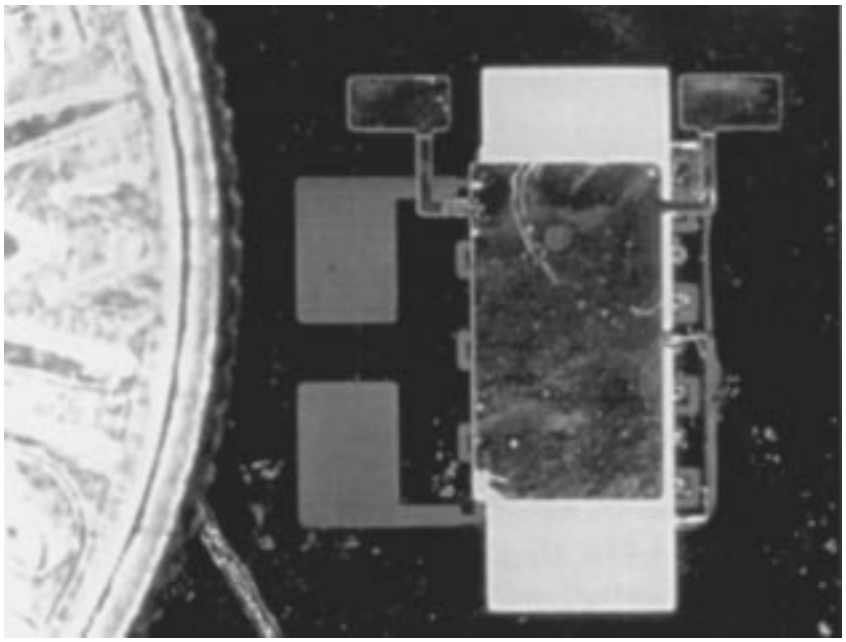

Fig. 4. Photomicrograph of a cantilever microrelay which had an actuation power of 33 mW.

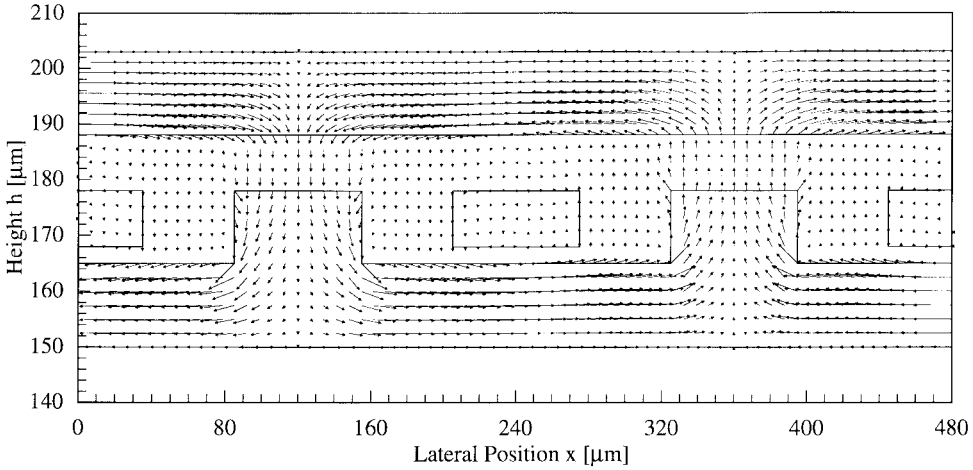

Fig. 5. Vector plot of the magnetic induction B in a cross section of the microrelay as obtained from a 2-D magnetic FE simulation.

an infinite extension of the air above and below the actual microrelay structure. Initial simulations were based on the nonlinear material properties of the permalloy films as measured with a vibrating sample magnetometer [21], [22]. After verifying that the NiFe cores are not saturated during device operation, all of the following magnetic simulations were performed assuming linear material properties with an effective permeability $\mu_r = 300$ for permalloy. A permeability $\mu_r = 300$ for permalloy represents the lower values reported in the literature [21].

Fig. 5 shows a vector plot of the resulting magnetic induction B in the microrelay as calculated from the 2-D model. The air elements above and below the relay structure are not displayed for clarity. Clearly visible is the characteristic alternating flux pattern obtained for the single layer coil structures: whereas the magnetic field direction is "downward" within one of the side cores, it is "upward" in the next side core. Within each side core, the field components created by the adjacent current lines are additive. For typical microrelay dimensions and a driving current $I = 1$ A, a maximum magnetic induction on the order of $B = 0.15$–0.25 T was obtained in the NiFe core below the current lines as well as in the upper plate above the coil lines. At the same time, the maximum magnetic field H in the air gap between the side cores and the upper plate was typically on the order of 450–600 Oersted ($H = 36\,000$–$48\,000$ A/m). The global force generated on the upper plate has been calculated within the ANSYS simulations using magnetic virtual displacement (MVDI) loading [23]. For a magnetic gap of 10 μm between the side cores and the upper plate, the available actuation forces F per area A typically range from $F/A = 300$–500 N/m^2 for the devices investigated in this work. The resulting forces are in general agreement with the actuation forces obtained from the analytical model based on standard reluctance theory [14].

Fig. 6 shows the FE model of the basic repeating unit of the zig–zag coil used for the 3-D simulations. For clarity reasons,

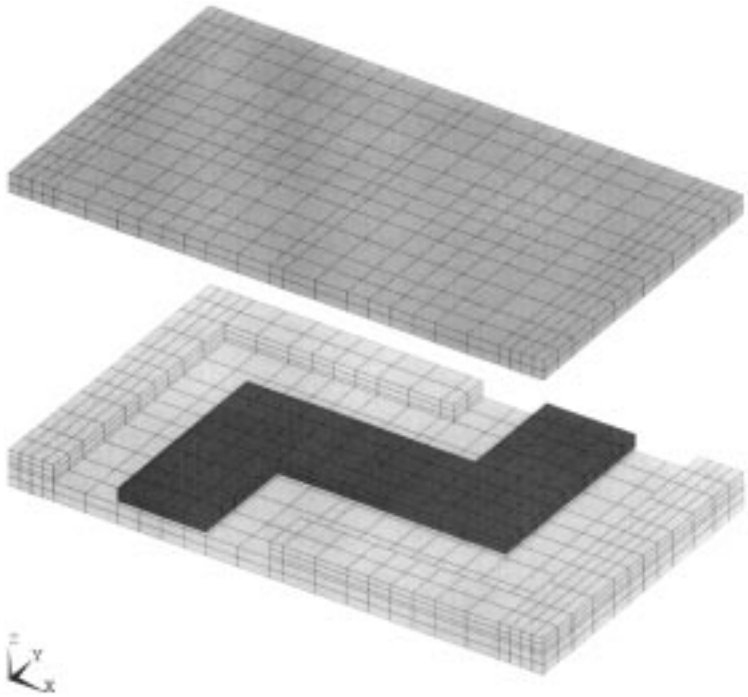

Fig. 6. Finite-element model of the basic repeating unit used for the 3-D magnetic simulation of the microrelay. For clarity reasons, only the core, coil, and upper plate are shown.

only the coil elements as well as the NiFe core elements are shown. Including the air and polyimide elements in the air gap as well as above and below the microrelay, the complete FE model consists of 6900 *eight-node magnetic solid* elements with three degrees of freedom (for the vector potential A) per node. Whereas flux-parallel boundary conditions (i.e., no flux is passing through the boundary plane) are applied along the boundaries to the neighboring coil elements, *3-D infinite boundary* elements available in the ANSYS program have been used to model the infinite extension of the air above and below the relay structure. Current is applied to the copper elements as a constant body load. Similar to the 2-D simulations, the forces acting on the magnetic upper plate have been calculated using MVDI loading.

In the following, the principal results of the 3-D simulations are discussed for the relay design shown in Fig. 4. The basic repeating unit of the coil design has lateral dimensions of 240 by 420 μm. The actuation force has been calculated as a function of the coil current and the magnetic gap g between the top of the side cores and the bottom of the upper plate. The upper plate touches the contacts for a magnetic gap $g = 10$ μm due to the fact that the planarization layers and the contacts are between the electromagnet and upper plate. Fig. 7 shows the force generated on the upper plate of the repeating unit (with area $A \approx 100 \times 10^{-9}$ m^2) as a function of the magnetic gap g for different driving currents. The upper plate of Fig. 5 with its lateral dimensions of 3.5 by 1.95 mm covers 68 repeating units. The actuation force increases with the square of the coil current as expected from the reluctance theory. The dependence of the force on the spacing between side cores and the upper plate can roughly be described by a power law $F \sim g^n$ (solid lines in Fig. 7) with an exponent $n \approx -1.4$. This result is in

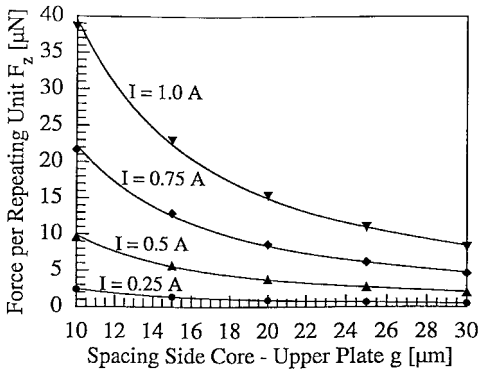

Fig. 7. Simulated force on the upper plate of the basic repeating unit as a function of the magnetic gap between side cores and upper plate for different actuation currents—the upper plate touches the contacts for a magnetic gap $g = 10$ μm.

contrast to the analytical model based reluctance theory which predicts $n = -2$, but does not account for the reluctance of the core and the 3-D nature of the coil design. Assuming that the upper plate is completely pulled down to the contacts (i.e., $g = 10$ μm), the total magnetic force acting on the upper plate is 2.5 mN for a coil current $I = 1$ A. This corresponds to a force per actuator area of $F/A = 380$ N/m^2. As will be seen in the following section, these large forces imply that currents much smaller than 1 A will be required for relay actuation.

Based on the actuation forces calculated in the magnetic analysis, a structural analysis of the upper plate was performed to predict its deflected shape as well as the contact forces. The upper plates have been modeled using *four-node structural shell* elements. A Young's modulus of $E = 80$ GPa, which represents the results of several investigations for thin electroplated permalloy films [24], [25], was used in the simulations.

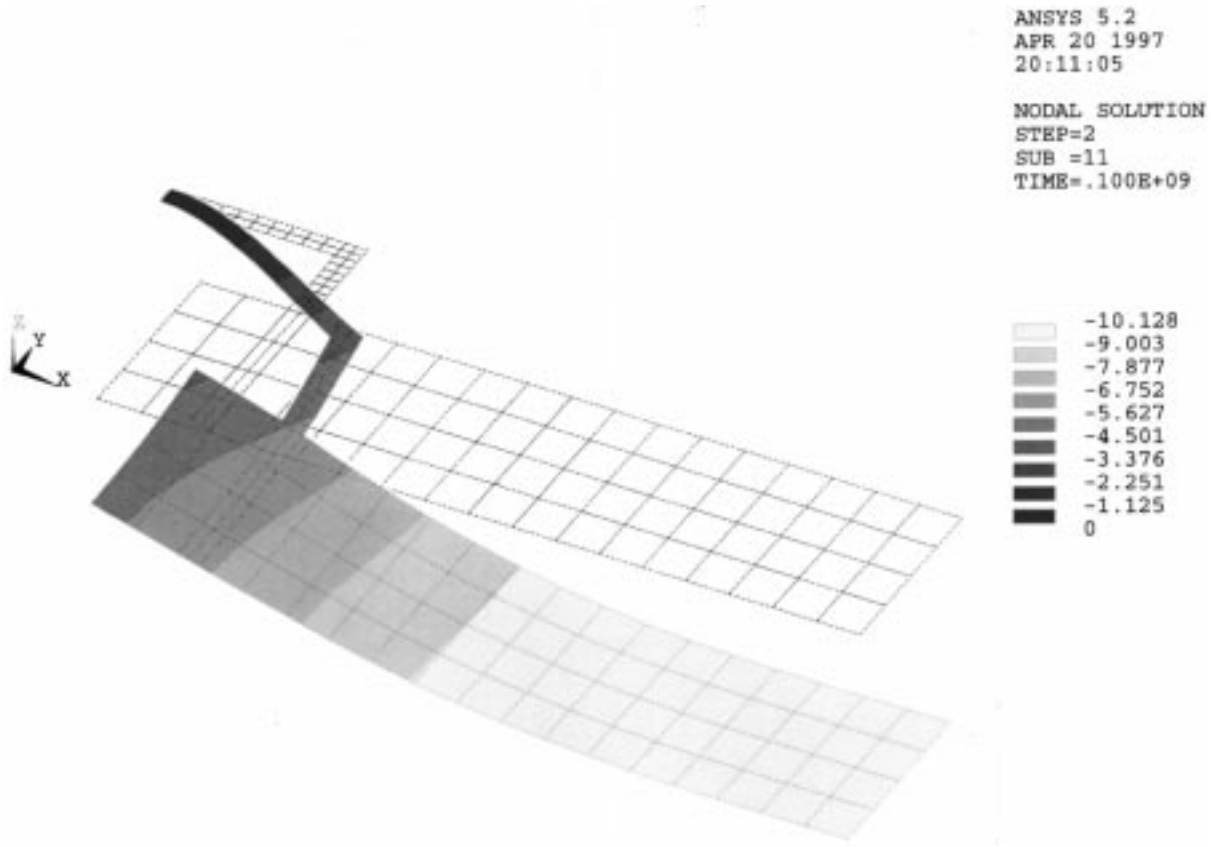

(a)

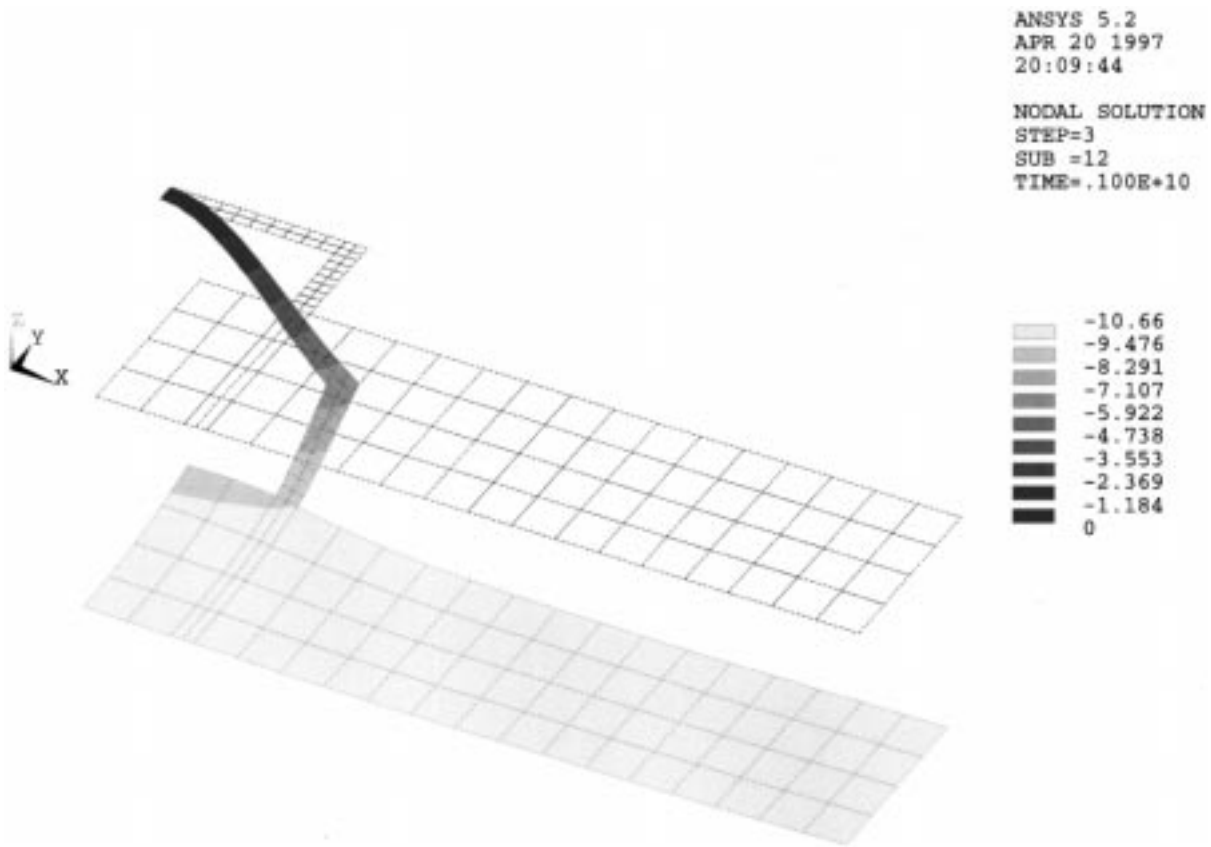

(b)

Fig. 8. Simulated deflection of the 10-μm-thick upper plate of the relay shown in Fig. 4 subject to a distributed force of (a) $F = 0.1$ mN and (b) $F = 1.0$ mN.

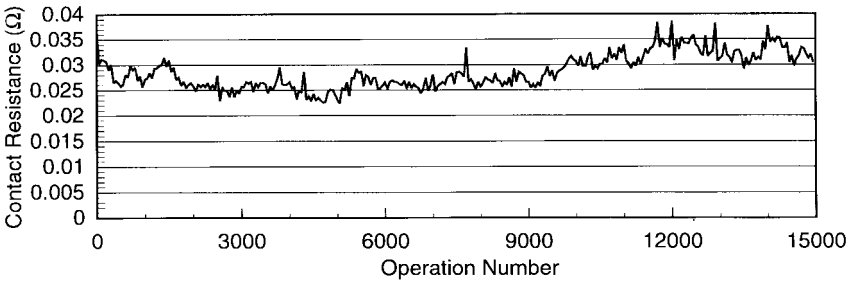

Fig. 9. Contact resistance of microrelay as measured using a four-terminal method. The maximum contact resistance measured was 38.6 mΩ, and the minimum contact resistance measured was 22.4 mΩ. Testing was stopped arbitrarily, not due to device failure.

Additional *3-D contact elements* between the upper plate and a rigid substrate allow the simulation of the microrelay contact in a nonlinear structural analysis. In this work, a constant pressure has been applied to all the elements of the upper plate (except the beam suspensions), although the actual force acting on each element depends on its distance from the coil. However, if the upper plate is completely pulled down, the magnetic force per area is indeed constant across the upper plate. Within the nonlinear analysis, the total force acting on the upper plate is ramped to its final value with two load steps. In the first load step, the force is increased in very small increments until the upper plate touches the contacts at the beam tip. As soon as this contact is established, the overall stiffness of the upper plate to transverse loads strongly increases. In the next load step, the force is ramped to its final value. Typically, the load is increased in 40 substeps to the final value. As an example, Fig. 8(a) and (b) shows the deflection of the relay upper plate of Fig. 4 (assuming a plate thickness of 10 μm) for actuation forces of $F = 0.1$ and 1 mN, respectively. Whereas about half of the upper plate is making contact to the substrate for $F = 0.1$ mN, the upper plate is almost completely pulled down for $F = 1$ mN. An actuation force of $F = 0.1$ mN is already achieved with a coil current of about 200 mA. These results demonstrate that reliable relay operation can be achieved for operating currents below 200 mA.

In addition, the structural ANSYS simulation gives an estimation for the achievable contact forces. If the 3.5 by 1.95-mm upper plate structure described above is pulled down with a total force of 1 mN [see Fig. 8(b)], the total contact force is about 0.9 mN. A separate structural analysis of the suspension beams indicates that a force of only 0.06 mN per beam is required to deflect its tip by 10 μm.

Modal analysis of the movable plate was performed in order to determine the resonance frequency of the upper plate structure. *Four-node plastic shell* elements with six degrees of freedom at each node were used to model the upper plate geometry. The first resonance frequency was calculated as 166 Hz for the structure of Fig. 4.

V. Results

Several different relay geometries were tested. These included four-arm bridge-type upper movable plates and more flexible two-arm cantilever-type upper plates and two coil designs with different repeating unit sizes. In addition, two operating modes of the relay were investigated: one in which the movable plate formed one of the contacts and one or both of the lower contacts formed the second contact (mode 1) and one in which the movable plate bridged both lower contacts (mode 2). The first operation mode had lower contact resistance since only one contact to movable plate interface is formed upon relay closure—the second operation mode had higher contact resistance, but no current must flow through the movable plate support arms.

A. Coil and Actuation Tests

All types of suspensions, coils, and operating modes produced successfully actuating and functional relays. As expected, the more flexible cantilever-type suspension combined with a tighter coil spacing resulted in lower actuation currents. The first operation mode had lower contact resistance when compared to the second operation mode. For a typical cantilever-type device, with beam dimensions of 200-μm width and 2-mm length, actuation was achieved with a 500-mA coil current. The lowest contact resistance was observed at 600 mA for these devices—the actuation power (i.e., power consumed by the coil) was 320 mW at the 600-mA actuation current. By decreasing the line width of the coils and increasing the number of coil lines under the upper plate, actuation currents and powers of 180 mA and 33 mW, respectively, were achieved. Fig. 4 is a photomicrograph of the minimum actuation power device. Other geometric parameters of the power-minimized device were beam widths of 100 μm and an upper plate that was 1.95 $\times$ 3.5 mm in length. These power levels are more typical of commercially available reed and miniature armature relays, which are typically rated at 50–100 mW of coil power.

The coil resistance of the microrelays was typically 1–1.5 Ω, depending on coil size and thickness. The microrelay coils have been tested up to and in excess of 3.0-A dc continuously for several hours and did not fail. The coil and relay were both still operational after this experiment.

The voltage isolation between the coil and the contacts was also tested. The fixed lower contact was used as one terminal, and the coil as another. Voltages up to 1600 V show no signs of dielectric breakdown. Typical miniature armature relays must maintain 1500-V isolation between coil and contacts.

B. Contact Resistance Tests

Measurements of the microrelay contact resistance (defined as the resistance from one bonding pad of the relay contact to the other bonding pad, including the interface resistances)

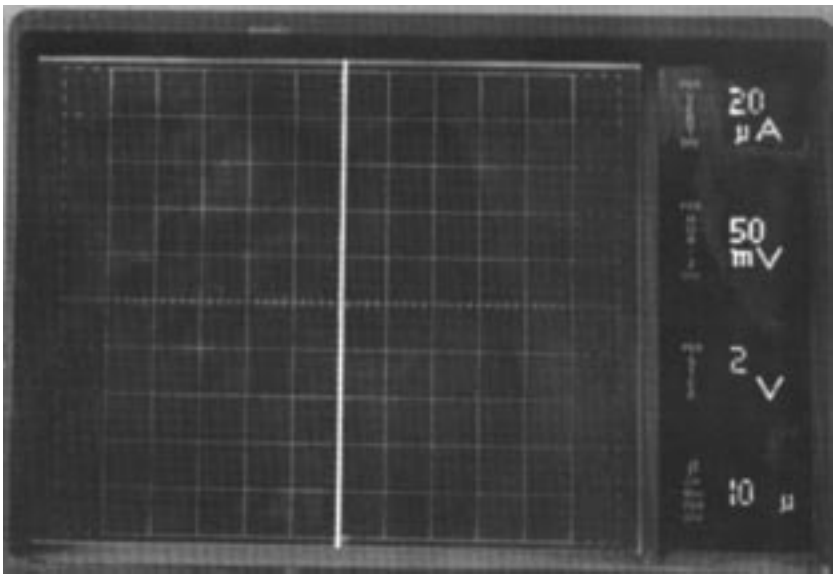

Fig. 10. Photograph of curve tracer output for low-level load. Vertical axis is 20 μA/div, and the horizontal axis is 50 mV/div.

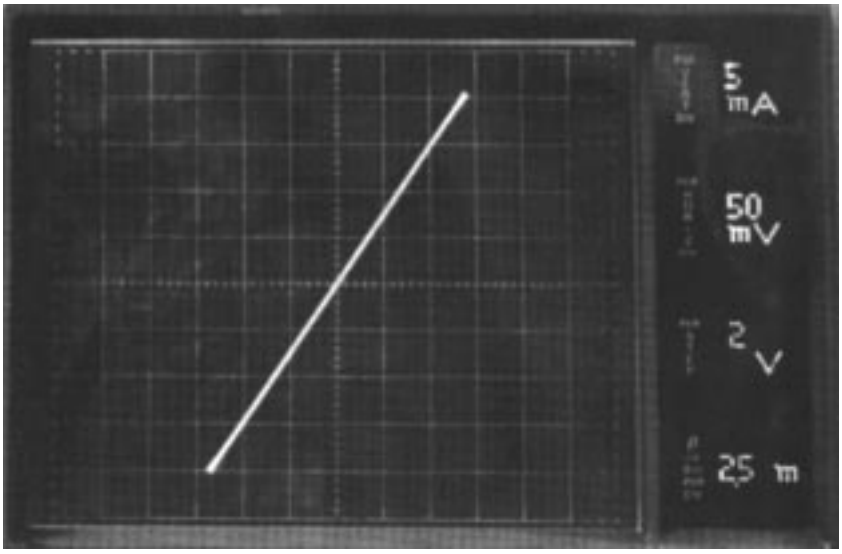

Fig. 11. Photograph of curve tracer output for higher current load. Vertical axis is 5 mA/div, and the horizontal axis is 50 mV/div.

under electromagnetic actuation were performed in air using a dc multimeter. Values of the "ON" resistance as low as 22.4 mΩ were measured using a four-point probe technique, with the maximum value observed over 15 000 operations being 38.6 mΩ. Fig. 9 shows the contact resistance versus trial for the 15 000 operations. Testing was stopped arbitrarily, not due to any change in device performance. The "OFF" resistance was infinite—no current flow was observed with voltages in excess of 10 V applied across the contacts. The contact materials were gold in these relays.

Contact resistance was also measured on a curve tracer in order to determine if the contact resistance was constant at low-level loads for the nickel–iron to gold contacts. Fig. 10 is a photograph of the curve tracer display with the y axis being 20 μA/div and the horizontal axis being 50 mV/div. Fig. 11 is a photograph of the curve tracer display for a y axis of 5 mA/div and an x axis of 50 mV/div. Clearly, in Figs. 10 and 11, the current-voltage behavior is linear at both low and high currents. This should allow for these devices to be used in low signal switching applications.

C. Switching Current Tests

Testing of a microrelay with an active load being switched across the contacts has also been performed. A cantilever-type microrelay, shown in Fig. 12, was able to repeatedly switch a 1.2-A dc load, both making and breaking the circuit in the first operational mode (one contact to upper plate interface) by energizing the relay coil. The voltage across the microrelay contacts when the relay was open was 3.0 V. This relay had an upper plate measuring 4 mm $\times$ 2.4 mm. The suspension arms were 400 μm wide. The voltage drop across the contacts was measured to be 1.6 V at the 1.2-A current. Thus, the contacts

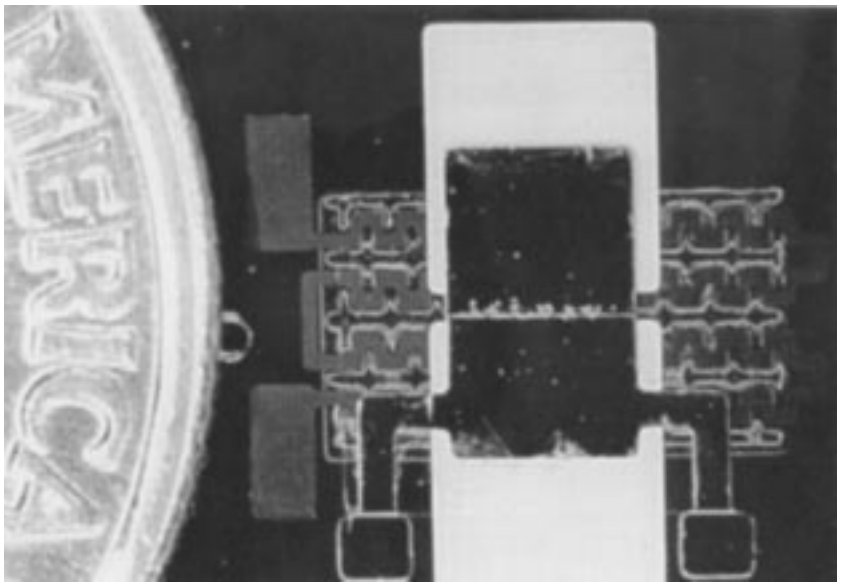

Fig. 12. Photomicrograph of a cantilever microrelay shown next to a dime. This type of relay has been able to switch 1.2 A by means of electromagnetic actuation of the upper plate using the integrated electromagnet.

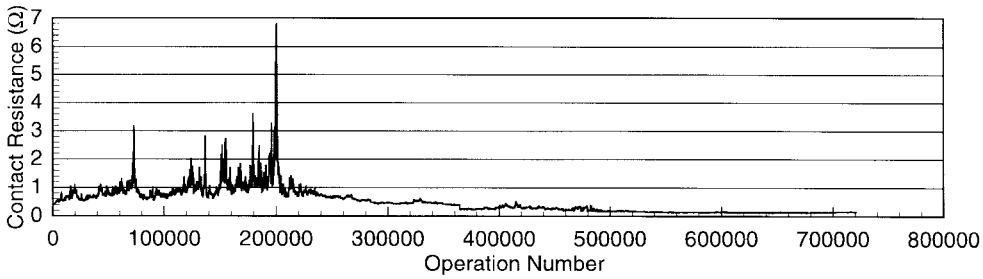

Fig. 13. Lifetime result of a microrelay shown to 700 000 plus operations. This device was tested in laboratory air in an unpackaged state. Testing was stopped arbitrarily, not due to any changes in device performance.

were able to successfully operate with 1.92 W of power being dissipated across them without contact failure. No experiments were conducted beyond 1.2 A with electromagnetic actuation.

Testing of the microrelay contacts for their ultimate limits was performed using mechanical actuation of the microrelay instead of electromagnetic actuation. The contacts when closed mechanically (nonswitching) had a contact resistance of 0.017 Ω and could carry 4.5 A of current for several minutes before failure occurred and 3 A of current repeatedly without failure.

D. Lifetime Tests

A long-term reliability test of the microrelay was performed using a computer-controlled actuation and measurement setup. The current passed through the microrelay contacts during these tests was supplied by a digital multimeter (DMM) in the resistance measurement mode, and was approximately 2.5 mA. The voltage across the contact when the relay was off (contacts open) was also provided by the DMM and was nominally 5 V. The devices tested have shown that operation lifetimes in excess of 850 000 cycles are possible. Tests beyond 850 000 cycles were not performed, and the termination after 850 000 cycles was arbitrary, not due to any changes in device performance. Fig. 13 shows lifetime test results for a cantilever-type device, with gold–gold contact material. The test was performed using a two-wire technique, and thus the influence of the test leads affected the measurements. A four-point technique was then used to measure the resistances more accurately as reported above. The device was tested in an unpackaged state and was not protected from dust or other disturbances in the surrounding air.

E. Switching Speed Tests

Actuation times of the microrelays were typically in the range of 0.5–2.5 ms, with values as large as 5 ms being observed for some of the microrelays. The differences in the actuation times arise from the different mechanical structures of the upper magnetic plates used for different micromachined relays. Fig. 14 shows a typical switching time measurement. This particular measurement was taken with a 5.1-kΩ resistive

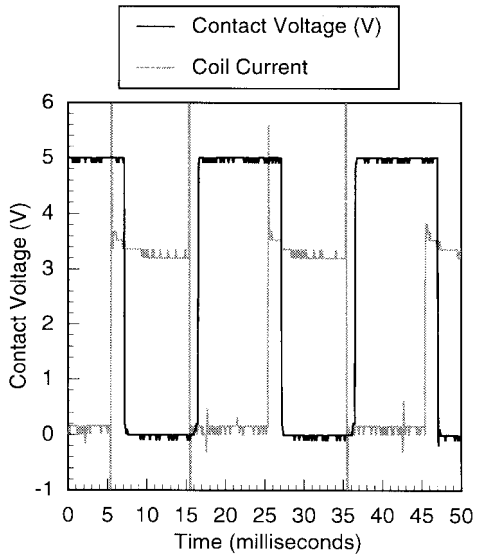

Fig. 14. Switching speed diagram for a typical fully integrated magnetic microrelay. The graph shown is a for a driving frequency of 50 Hz and 5-V dc applied across the open contacts.

load on the contacts and a driving frequency of 50 Hz with 5 V being applied across the contacts when they were open. The driving current is relatively high, in excess of 1.5 A, however, this device was not optimized for minimum driving current. No coil-suppression diodes were used on the coil driving circuit. There was little or no bounce observed in these devices, which is understandable due to the low mass and, therefore, low inertia of the moving plate. The reduction of bounce will allow for longer lifetimes for two reasons—the number of arcs should be reduced because if arcing occurs it will occur only once per switch closure, and the amount of mechanical abrasion between the two contacts surfaces will be reduced as they only meet once during the switching cycle. Typical release times were measured to be 2.5 ms, with values as low as 0.9 ms being observed. Microrelays have successfully opened and closed at a frequency of 1 kHz with resistive loads. Other loads were switched by the microrelays including LED's and inductive loads of 1.8 mH.

VI. Conclusions

Fully integrated magnetically actuated micromachined relays have been realized. Through minimization of the coil design, the power required for switching has been reduced to 33 mW. Microrelays have been fabricated which can switch up to 1.2 A electromagnetically without device failure. Contact resistances below 50 mΩ were observed repeatedly. Lifetime testing of the microrelays has shown that devices remain operational after 850 000 operations. FE simulations indicate that actuation forces on the order of several millinewtons can be achieved for this type of microrelay with a single-layer coil. Since the typical force required for actuation is on the order of 0.1 mN, a contact force in excess of 1 mN should be achievable.

Acknowledgment

The authors would like to acknowledge C. Dauwalter and Y.-J. Kim for valuable technical discussions.

References

[1] K. E. Petersen, "Membrane switches on silicon," *IBM J. Res. Develop.*, vol. 23, pp. 376–385, 1979.

[2] M. A. Gretillat, P. Thieubaud, N. F. de Rooij, and C. Linder, "Electrostatic polysilicon microrelays integrated with MOSFET's," in *Proc. IEEE Microelectromechanical Syst. Conf.*, Oiso, Japan, 1994, pp. 97–101.

[3] M. A. Gretillat, P. Thieubaud, C. Linder, and N. F. de Rooij, "Integrated circuit compatible electrostatic polysilicon microrelays," *J. Micromech. Microeng.*, vol. 5, pp. 156–160, 1995.

[4] S. Roy and M. Mehregany, "Fabrication of electrostatic nickel microrelays by nickel surface micromachining," in *Proc. IEEE Microelectromechanical Syst. Conf.*, Amsterdam, The Netherlands, 1995, pp. 353–357.

[5] J. Drake, H. Jerman, B. Lutze, and M. Stuber, "An electrostatically actuated microrelay," in *Proc. Transducers'95*, Stockholm, Sweden, vol. 2, pp. 380–383.

[6] M. Sakata, "An electrostatic microactuator for electromechanical relay," in *Proc. IEEE MEMS Workshop*, Salt Lake City, UT, 1989, pp. 149–151.

[7] J. J. Yao and M. F. Chang, "A surface micromachined miniature switch for telecommunication applications with signal frequencies from dc up to 4 GHz," in *Proc. Transducers'95*, Stockholm, Sweden, vol. 2, pp. 384–387.

[8] P. M. Zavracky, S. Majumder, and N. E. McGruer, "Micromechanical switches fabricated using nickel surface micromachining," *IEEE J. Microelectromech. Syst.*, vol. 6, no. 1, pp. 3–9, 1997.

[9] H. F. Schlaak, F. Arndt, J. Schimkat, and M. Hanke, "Silicon-microrelay with electrostatic moving wedge actuator—New functions and miniaturization by micromechanics," in *Proc. 5th Int. Conf. Micro Electro, Opto, Mechanical Syst. Components*, 1996, pp. 463–468.

[10] J. Simon, S. Saffer, and C. J. Kim, "A micromechanical relay with a thermally-driven mercury micro-drop," in *Proc. IEEE Microelectromechanical Syst. Conf.*, San Diego, CA, 1996, pp. 515–520.

[11] H. Hosaka, H. Kuwano, and K. Yanagisawa, "Electromagnetic microrelays: Concepts and fundamental characteristics," in *Proc. IEEE Microelectromechanical Syst. Conf.*, Ft. Lauderdale, FL, 1993, pp. 12–17.

[12] ———, "Electromagnetic microrelays: Concepts and fundamental characteristics," *Sens. Actuators A (Physical)*, vol. A40, pp. 41–47, 1994.

[13] E. Hashimoto, H. Tanaka, Y. Suzuki, Y. Uenishi, and A. Watabe, "Thermally controlled magnetization actuator (TCMA) using thermosensitive magnetic materials," in *Proc. IEEE Microelectromechanical Syts. Conf.*, Oiso, Japan, 1994, pp. 108–113.

[14] W. P. Taylor, M. G. Allen, and C. R. Dauwalter, "A fully integrated magnetically actuated micromachined relay," in *Proc. 1996 Solid State Sensor and Actuator Workshop*, Hilton Head, SC, 1996, pp. 231–234.

[15] C. H. Ahn and M. G. Allen, "A planar micromachined spiral inductor for integrated magnetic microactuator applications," *J. Micromech. Microeng.*, vol. 3, pp. 37–44, 1993.

[16] A. B. Frazier, C. H. Ahn, and M. G. Allen, "Development of micromachined devices using polyimide-based processes," *Sens. Actuators A (Physical)*, vol. A45, pp. 47–55, 1994.

[17] A. B. Frazier and M. G. Allen, "Metallic microstructures fabricated using photosensitive polyimide electroplating molds," *IEEE J. Microelectromech. Syst.*, vol. 2, no. 2, pp. 87–94, 1993.

[18] T. Imagawa, M. Sano, S. Narishige, and M. Hanazono, "Thermal stability of magnetic properties of electroplated Ni-Fe-In ternary alloy films," *Trans. Magn.*, vol. 22, pp. 629–631, 1986.

[19] A. S. Kao and P. Kasiraj, "Effect of magnetic annealing on plated permalloy and domain configurations in thin-film inductive head," *Trans. Magn.*, vol. 27, no. 6, pp. 4452–4457, 1991.

[20] Z. Nami, C. Ahn, and M. G. Allen, "An energy-based design criterion for magnetic microactuators," *J. Micromech. Microeng.*, vol. 6, pp. 337–344, 1996.

[21] M. Schneider, R. Castagnetti, M. G. Allen, and H. Baltes, "Integrated flux concentrator improves CMOS magnetotransistors," in *Proc.*

IEEE Microelectromechanical Syst. Conf., Amsterdam, The Netherlands, 1995, pp. 151–156.

[22] W. P. Taylor, M. Schneider, H. Baltes, and M. G. Allen, "Electroplated soft magnetic materials for microsensors and microactuators," in *Proc. Transducers'97,* Chicago, IL, 1997, pp. 1445–1448.

[23] *Ansys 5.2 Users Manual,* Swanson Analysis, Inc., Houston, PA.

[24] C. C. Chung and M. G. Allen, "Measurement of mechanical properties of electroplated nickel–iron alloys," in *Proc. 1996 Int. Mechanical Eng. Congress and Exposition,* Atlanta, GA, pp. 453–457.

[25] J. A. Wright, Y. Tai, and S. Chang, "A large-force, fully integrated MEMS magnetic actuator," in *Proc. Transducers'97,* Chicago, IL, vol. 2, pp. 793–796.

William P. Taylor (S'89–M'98) received the B.E.E. degree in 1993, the M.S. degree in 1995, and the Ph.D. degree in electrical engineering in 1997, all from the Georgia Institute of Technology, Atlanta.

His research has focused on the development of magnetically actuated micromachined relays. He also has worked on electroplated magnetic materials for microsensor and microactuator applications. In 1998, he joined Teledyne Relays, Hawthorne, CA.

Oliver Brand received the M.S. degree in physics from the Technical University Karlsruhe, Germany, and the Ph.D. degree from ETH Zurich (Swiss Federal Institute of Technology), Switzerland, in 1990 and 1994, respectively.

From 1995 until 1997, he was a Post-Doctoral Fellow at the Georgia Institute of Technology, Atlanta. Currently, he is a Senior Scientist at the Physical Electronics Laboratory, ETH Zurich. His research interest includes the development of microsensors and microactuators using industrial IC processes in combination with postprocessing micromachining steps.

Mark G. Allen (M'89) received the B.A. degree in chemistry, the B.S.E. degree in chemical engineering, and the B.S.E. degree in electrical engineering, all from the University of Pennsylvania, Philadelphia, in 1984, and the M.S. and Ph.D. degrees from the Massachusetts Institute of Technology (MIT), Cambridge, in 1986 and 1989, respectively.

Since 1989, he has been on the faculty of the School of Electrical and Computer Engineering, Georgia Institute of Technology, Atlanta, where he currently is Associate Professor. His research interests include micromachining fabrication technology, magnetic micromachined devices and systems, and materials issues in micromachined structures and electronic packages.

Dr. Allen was Cochair of the 1996 IEEE Microelectromechanical Systems Conference and is a Member of the Editorial Board of the Journal of Micromechanics and Microengineering.